Accurate Thickness Measurement of Multiple Coating Layers on Carbon Fiber Composites Using Microwave Cavity Perturbation

Zhen Li, Changcheng Wu, Zhaozong Meng, *Member, IEEE*, Constantinos Soutis, Zhijun Chen, Ping Wang, Andrew Gibson, *Senior Member, IEEE*

***Abstract*— Current techniques for evaluating the multi-layered coating thickness on carbon fiber-reinforced polymer composites are sub-optimal; here we present a new non-destructive microwave method using an open cavity resonator sensor. When the open end of the cavity is positioned on a conductive polymer composite a resonant cavity is formed. The coating perturbs the surface impedance, causing resonance frequency shift. In the modelling, the original endplate perturbation theory for a closed resonant cavity is modified, incorporating the effect of the coating. One-, two- and multi-layered coating cases are studied, and a linear relationship is revealed between the resonance frequency shift and the coating thickness change. The accuracy of the model is confirmed by electromagnetic simulation performed with CST software and actual measurements. It is shown that the proposed sensor is insensitive to the conductivity anisotropy of the composite examined, offering easy implementation. For the coating thickness estimation, errors within ±5% have been observed, where two reference cases are used as a simple form of calibration. The methodology presented here offers efficient on-site evaluation of coatings on composite structures of aircraft and other applications.**

***Index Terms*— analytical model, cavity perturbation, thickness measurement, multiple coatings, composites**

I. INTRODUCTION

Carbon fiber-reinforced polymer (CFRP) composites have been widely employed in aircraft structures (e.g., fuselage and wings) for the high strength-to-weight ratio and stiffness-to-weight ratio [1]. For aesthetics and performance purposes, the aircraft exterior is commonly painted with multiple coating layers. For example, the top coating (also called topcoat) is used to withstand ultraviolet exposure at cruise altitudes, and the bottom coating (primer) is applied to bond to the surface. All the coatings are required to sustain the extreme temperature cycles during the flight. Due to size and shape complexity of the structure, painting is generally performed by manual spraying, especially if this is a repainting job. Thickness variation by this operation is inevitable but it should not be out of the allowable range, otherwise causing either degraded performance or overweight. The conventional weighing approach is time-consuming and lacks local thickness details. The drilling method is destructive and cannot be used for in-field tests. Thus, more efficient coating thickness measurement is of great demand. It is noted that very few of the existing non-destructive testing (NDT) methods can be employed. For example, the composite is not translucent, so the optical methods (e.g., spectral interferometry) cannot be employed. Eddy current testing and magnetic induction can only be used for metallic bases [2]. Methods like terahertz testing [3] and X-ray fluorescence [4] are limited to laboratory use due to the intricate instrumentation. Ultrasonic scanning needs couplants to eliminate signal loss in the air. Thorough cleaning of the couplants is a must, as any residue can affect the painting of the next layers. For guided waves, several transducers should be bonded on the surface, so the same cleaning problem exists. When the total coating thickness needs checking after the painting of each layer, this type of setup becomes ineffective and not practical. Hence, there is a continuing search for alternative methods that could offer improved evaluation.

In recent years, microwave testing has received considerable attention for the advantages of easy implementation and desired applicability for composites. In the test, the sensor is placed on the coating with no need for couplants, as the microwave signals propagate well in low-loss materials like air and coating. The composites behave more similar to metals over microwaves than the radio frequency range used in the eddy current testing, facilitating the analysis of the electromagnetic responses in the substrate. In addition, the microwave technique has no ionizing radiation hazards and requires low signal power consumption (in the range of milliwatts) [5]–[7]. The microwave sensors for coating thickness measurement on composites can be classified into three types: an open-ended waveguide [8], an open cavity resonator [9]–[11] and an open-ended coaxial probe [11], [12]. For the first approach, an analytical model describing the radiation from the waveguide aperture into stratified dielectrics was adopted for the inverse

This manuscript was submitted on 20 October 2021. This work was supported in part by the Natural Science Foundation of Jiangsu Province (Grant No. BK20200427), the National Natural Science Foundation of China (Grant No. 52105552), and the Shuangchuang Project of Jiangsu Province (Grant No. KFR20020).

Z. Li, C. Wu, Z. Chen and P. Wang are with College of Automation Engineering, Nanjing University of Aeronautics and Astronautics, Nanjing, 200106, China (Corresponding author: Z. Li, e-mail: zhenli@nuaa.edu.cn).

Z. Meng is with School of Mechanical Engineering, Hebei University of Technology, Tianjin, 300401, China.

C. Soutis is with Aerospace Research Institute, The University of Manchester, Manchester, M13 9PL, UK.

A. Gibson is with Faculty of Science and Engineering, Manchester Metropolitan University, Manchester, M1 5GD, UK.

problem. The dielectric properties of the coating were measured first, and calibration using commercial calibration kits was required to shift the reference plane to the aperture. A simple scenario with one dielectric sheet on a woven composite plate was studied and the estimation error was up to 15%. Special attention should be paid to the probe placement with respect to the fiber directions for other composite types, as the electric fields inside the waveguide are polarized. For the resonator and coaxial probe, only experimental work was reported. Coatings or foils with known thicknesses were measured to obtain calibration curves. For the three types of sensors, extensive calibration is required, involving varied combinations of coatings and composites that can occur in practice.

In this paper, a new microwave measurement strategy with little dependence on calibration is presented for multi-layered coating cases, where an analytical model is proposed using the modified cavity perturbation theory. The resonance frequency shifts in the no-coating, one-, two- and multi-layered coating cases are studied in detail. An open cylindrical cavity resonator sensor is developed, and electromagnetic simulation is performed first for preliminary verification of the model. Then, experiments are carried out, where the effects of the coating thickness, coating material, substrate conductivity and resonant mode are thoroughly investigated.

II. Analytical Modelling

A. Cavity perturbation theory

A closed cylindrical cavity resonator is made from a section of a circular waveguide shorted at both ends. A closed resonant system can also be formed when an open cavity is in contact with a conductive plate. The endplate perturbation theory [13], [14] is employed for the analysis, where one endplate is replaced by another one while the cavity shape is kept unchanged. Here the resonant responses for the composite substrate with two different coating thicknesses are compared: one as the reference (or original) case and the other one as the perturbation case.

As illustrated in Fig.1, for the original cavity, the complex angular frequency can be represented by $\omega_a=2\pi f_{r,a}+j\pi f_{r,a}/Q_a$, where $f_{r,a}$ and Q_a are the resonance frequency and quality factor, respectively. After the perturbation, the complex angular frequency, resonance frequency and quality factor are changed to ω_b, $f_{r,b}$ and Q_b, respectively. Assuming that in most of the cavity volume the electric and magnetic field intensities remain the same due to small perturbation ($f_{r,a}\approx f_{r,b}$), the change of the complex angular frequency can be estimated by [15]

$$\begin{aligned}\omega_b-\omega_a &\approx 2\pi\left(f_{r,b}-f_{r,a}\right)+j\pi\left(\frac{f_{r,b}}{Q_b}-\frac{f_{r,a}}{Q_a}\right)\\ &\approx j\xi\left(Z_{s,b}-Z_{s,a}\right)\end{aligned} \tag{1}$$

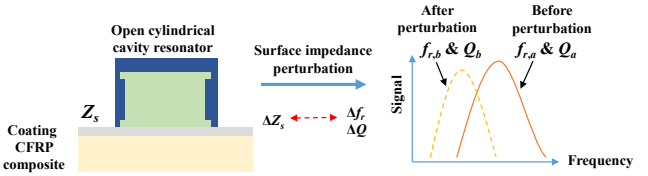

Fig.1 Illustration of the coating thickness measurement principle using microwave cavity perturbation.

where $Z_{s,a}$ and $Z_{s,b}$ are the surface impedances before and after the perturbation, respectively. ξ is a coefficient that can be given by

$$\xi=\frac{\int_S\left|\bar{E}_a\right|^2 ds}{\int_V\left(\varepsilon\left|\bar{E}_a\right|^2+\mu\left|\bar{H}_a\right|^2\right)dv} \tag{2}$$

where $\bar{E}_a$ and $\bar{H}_a$ are the electric and magnetic fields inside the original cavity, respectively. ε and μ are the electric permittivity and magnetic permeability of the medium in the cavity, respectively. Since the cavity used is air-filled, ε and μ are equal to the permittivity ε_0 and permeability μ_0 of free space, respectively. The surface integral is taken over the cavity walls, and the volume integral is taken over the cavity. For a specific mode, ξ can be treated as a positive constant.

B. No-coating case

The surface impedance of a non-magnetic conductive plate can be approximated by [16]

$$Z_s\approx(1+j)\sqrt{\frac{\pi\mu_0 f}{\sigma}} \tag{3}$$

where f is the operating frequency and σ is the effective conductivity.

If one endplate with σ_a is replaced by another endplate with σ_b, by substituting (3) into (1), the resonance frequency difference Δf_r can be expressed as

$$\Delta f_r=f_{r,b}-f_{r,a}\approx\frac{\xi}{2}\sqrt{\frac{\mu_0 f_a}{\pi}}\left(-\frac{1}{\sqrt{\sigma_b}}+\frac{1}{\sqrt{\sigma_a}}\right) \tag{4}$$

Hence, with a lower conductivity (e.g., when an uncoated metallic endplate is replaced by an uncoated composite plate), the resonance frequency will be shifted downwards.

C. One-layer coating case

In the present work, the sensor operates in the $TE_{01\ell}$ (ℓ=1, 2, 3, …,) mode, where the electric fields only exist in the plane transverse to the cylinder axis. In addition, circumferential currents flow in the cylindrical wall and endplates, so there is no contact problem between the cavity and the endplates. The electric field along the circumferential direction is uniform, so no special scheme is needed for the placement of the probe on an electrically anisotropic substrate. The endplate is at the node of the electric field along the axial direction. Hence, the field intensity inside the coating layer is small, and the fields in the thin coating can be approximated by those of the TE_{01} mode in a circular waveguide.

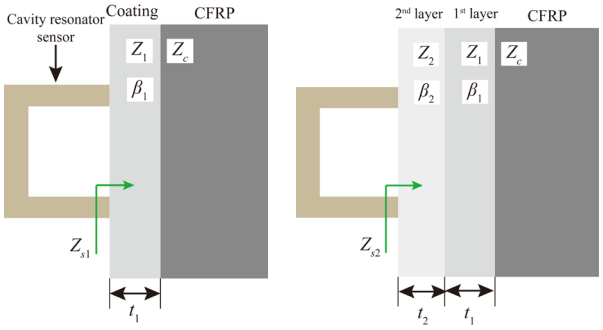

Fig. 2 Geometry for the modelling of the coating thickness measurement using an open cavity resonator: (a) one-layer case; (b) two-layer case.

For the one-layer coating case, as illustrated in Fig. 2 (a), the surface impedance is viewed as the input impedance Z_{s1} looking towards the coated composite. Here the thickness of the composite is considered infinitely large for the relatively low signal penetration depth inside the material.

Applying the transmission line theory, Z_{s1} can be expressed as

$$Z_{s1} = Z_1 \frac{Z_c + Z_1 \tanh \gamma_1 t_1}{Z_1 + Z_c \tanh \gamma_1 t_1} \tag{5}$$

where $\gamma_1=\alpha_1+j\beta_1$ is the complex propagation constant for the coating. α_1 is the attenuation constant and β_1 is the phase constant. γ_1 tends more imaginary as the coating is generally not lossy [17], [18]. t_1 is the coating thickness. Hence, $\tanh\gamma_1 t_1$ can be approximated by $j\tan\beta_1 t_1$. It is mentioned that the value of $\tan\beta_1 t_1$ is close to $\beta_1 t_1$, as the value of β_1 for the sensor developed is in the order of 10 m^{-1} and the value of t_1 is small (below 1 mm). Z_1 and Z_c are the wave impedances of the coating and composite, respectively. The electrical conductivity of the composite plate is significantly higher than that of the nonconductive coating [19], [20]. Therefore, from the definition of the impedance of the TE_{01} mode in a circular waveguide [21], Z_c is considerably lower than Z_1, so Z_{s1} can be approximated by

$$Z_{s1} \approx jZ_1\beta_1 t_1 \tag{6}$$

Z_1 can be written as

$$Z_1 = \frac{2\pi Z_0 f}{c\beta_1} \tag{7}$$

where Z_0 is the impedance of free space (i.e., 376.7 Ω), and c is the speed of light in free space. β_1 is a function of the permittivity of the coating. However, the product of Z_1 and β_1 generates a parameter that becomes independent of the permittivity. Accordingly, the expression of Z_{s1} can be further reduced to

$$Z_{s1} \approx \frac{2j\pi Z_0 f}{c} t_1 \tag{8}$$

By substituting (8) into (1), the relationship between the resonance frequency shift and coating thickness difference can be obtained

$$\Delta f_r \approx \kappa \Delta t = \kappa\left(t_{1,b} - t_{1,a}\right) \tag{9a}$$

$$\kappa = -\frac{\xi Z_0 f_a}{c} \tag{9b}$$

where κ is the coefficient for the linear correlation, and Δt is the coating thickness difference. $t_{1,a}$ and $t_{1,b}$ are the coating thicknesses in the original and perturbed cases, respectively. Dimensional homogeneity is confirmed using the dimensional analysis, and κ has a unit of Hz/m (an alternative unit MHz/μm is applied for easier analysis of the results unless mentioned otherwise). The resonance frequency decreases with increasing coating thickness, as the coefficient value is negative. By substitution no imaginary part appears on the right-hand side of (1), so the imaginary part related to the quality factors on the left-hand side is ignored. It is suggested that the model presented here can only be applied if the quality factor is not significantly changed after the perturbation, otherwise the assumption of small perturbation is no longer valid.

Theoretically, as the frequency shift shows insensitive to the coating and substrate types, a minimum of only two measurements are needed for the calculation of the κ value, e.g., using two dielectric foils with known thicknesses (same as the practice commonly adopted in the eddy current testing on a metallic substrate) or just one foil and the uncoated composite sample is chosen as the reference case. Certainly, multiple reference cases can be employed for more accurate determination by linear fitting. Alternatively, if two coating thicknesses are known in three different cases, $t_{1,c}$ for the third perturbation case can be readily computed without knowing the value of κ beforehand.

$$\frac{f_{r,c} - f_{r,a}}{f_{r,b} - f_{r,a}} \approx \frac{t_{1,c} - t_{1,a}}{t_{1,b} - t_{1,a}} \tag{10}$$

where f_c is the resonance frequency for the third perturbation case.

D. Two-layer coating case

By adopting the same methodology as the one-layer case, the surface impedance for the two-layer model (illustrated in Fig. 2 (b)) Z_{s2} can be expressed as

$$Z_{s2} = Z_2 \frac{Z_{s1} + Z_2 \tanh \gamma_2 t_2}{Z_2 + Z_{s1} \tanh \gamma_2 t_2} \approx jZ_2 \frac{Z_1\beta_1 t_1 + Z_2\beta_2 t_2}{Z_2 - Z_1\beta_1\beta_2 t_1 t_2} \tag{11}$$

where subscripts 1 and 2 correspond to the 1st and 2nd layers (counting from the substrate surface), respectively. Similarly, for the small values of t_1 and t_2, the term $Z_1\beta_1\beta_2 t_1 t_2$ can be omitted. Thus, the surface impedance Z_{s2} can be simplified as

$$Z_s \approx j\left(Z_1\beta_1 t_1 + Z_2\beta_2 t_2\right) = \frac{2j\pi Z_0 f}{c}\left(t_1 + t_2\right) \tag{12}$$

When t_1 or t_2 is equal to zero, (12) is reduced to (8). Therefore, the resonance frequency shift due to the thickness change can also be represented by (9) and (10). The only difference is that in the present case t_a, t_b and t_c denote the total thicknesses (e.g., $t_{1,a}$ is replaced by $t_{1,a}+t_{2,a}$). It is noted that the thickness of the topcoat t_2 cannot be readily extracted from the resonance frequency shift with respect to the no-coating case. Instead, the thickness of the primer t_1 can be computed first

using the one-layer model, as the primer is painted first. After the painting of the topcoat, the two-layer model can be introduced to calculate the total thickness. Then, the value of t_2 can be obtained by simple subtraction.

E. Multi-layered coating case

The analytical model can also be extended to a multi-layered coating case. By analogy, the surface impedance for the n-layer case Z_{sn} can be written as

$$Z_{sn} = Z_n \frac{Z_{s(n-1)} + Z_n \tanh \gamma_n t_n}{Z_n + Z_{s(n-1)} \tanh \gamma_n t_n} \approx \frac{2j\pi Z_0 f}{c} \sum_{m=1}^{n} t_m \quad (13)$$

where γ_n and t_n are the complex propagation constant and thickness for the n-th coating layer, respectively. $Z_{s(n-1)}$ corresponds to the surface impedance for the n-1 layers below the top layer. Z_{sn} is also proportional to the total thickness, so (9) and (10) can still be applied.

III. Sensor Design

The sensor structure is illustrated in Fig. 3, where an aluminum cylindrical wall is mechanically joined to an aluminum endplate by socket screws. The inner radius (r) and height (h) of the cavity are 47.5 mm and 40 mm, respectively. Two SubMiniature version A (SMA) connectors are mounted on the endplate. Small wire loops are used for signal coupling, and the $TE_{01\ell}$ mode can be excited by this approach. It is noted that the $TM_{11\ell}$ mode has the same frequency as the $TE_{01\ell}$ mode but exhibits different field distributions. To avoid the interference of the degenerate mode, small grooves are made at both the top and bottom edges of the cavity body. The grooves are at an anti-node of the TM mode but a node in the TE mode, so they have a larger effect on the TM mode and the corresponding resonance frequency decreases due to the larger diameter at the groove position. The resonance frequency of the $TE_{01\ell}$ mode in a closed air-filled cylindrical cavity can be calculated by

$$f_r = \frac{c}{2\pi} \sqrt{\left(\frac{p'_{01}}{r}\right)^2 + \left(\frac{\ell\pi}{h}\right)^2} \quad (14)$$

where p'_{01}=3.832 is the first root of the derivative of J_0. In this work, the TE_{011} (ℓ=1) mode is of primary interest, as the frequency difference with the adjacent modes is relatively large, thereby offering easy mode identification and a wide dynamic range for the measurement. By substituting the values of r and h, the theoretical f_r value of the TE_{011} mode is approximately 5.3721 GHz.

IV. Experimental Setup

The setup for the coating thickness measurement is presented in Fig. 4. The sensor was connected to a Fieldfox N9951A portable microwave analyzer (Keysight Technologies, Santa Rosa, CA) by two coaxial cables. The transmission coefficients S_{21} were retrieved from the analyzer to a personal computer (PC) by a LAN cable. The default setting of the signal power -15 dBm (i.e., 0.032 mW) was adopted. A factory calibration known as *CalReady* was automatically performed at the test port connectors of the analyzer when the analyzer was switched on. 401 frequency points over a span of 20 MHz was used, and the intermediate frequency bandwidth (IFBW) was set to 100 Hz to significantly reduce the noise floor and get accurate measurement of the S-parameter data.

Two 4 mm thick T300 CFRP composite samples were used, i.e., a plain woven plate and a unidirectional (UD) laminate. Commercially available polyethylene (PE), polyethylene terephthalate (PET), polyvinyl chloride (PVC) and Flame Retardant 4 (FR4) woven fiberglass-epoxy foils were used to simulate the coating. The thickness of a single foil was measured by a digital micrometer (Syntek Co., Ltd, Deqing, China), which had a resolution of 1 μm and an accuracy of ±2 μm. The thicknesses of PE, PET, PVC and FR4 were approximately 44 μm, 56 μm, 295 μm and 145 μm, respectively. Plastic pieces with dimensions larger than the cavity aperture were cut and stacked onto the substrate. The sensor was gently pressed against the foils to eliminate any air gap.

V. Results and Discussions

A. Electromagnetic simulation

Numerical simulation is performed using CST® software. The frequency domain solver is used, and the adaptive mesh refinement option is chosen to produce a fine mesh. The one-layer coating case is analyzed, and the simulation model generated is shown in Fig. 5 (a). Quartz and FR4 with known permittivity values ($3.75\text{-}j1.5\times10^{-3}$ and $4.3\text{-}j0.11$, respectively) from the built-in material library are chosen as the coating. As the properties of a composite are not readily available, the material of the substrate is defined as aluminium instead. The conductivity of aluminium is higher than that of the composite, so the analytical model can be applied as well. It is noted that only partial verification can be achieved by the simulation. More comprehensive examination using composites is done by experiments.

As presented in Fig. 5 (b), the resonance peak moves downwards with increasing thickness from 50 μm to 1 mm. Compared with the direct contact case, the resonance frequency change Δf_r at different layer thicknesses (t) is plotted in Fig. 6, where the points for quartz and FR4 overlap and good linear relationships are observed. Thus, regression analysis is employed here.

$$\Delta f_r = \kappa_1 t + \kappa_0 \quad (15)$$

where κ_0 and κ_1 are the regression constants. The high coefficients of determination (R^2=0.9999) imply good fitting.

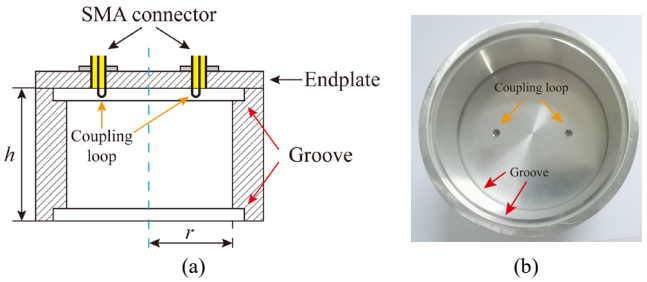

Fig. 3 Cavity resonator sensor developed for the coating thickness measurement: (a) cross section; (b) bottom view.

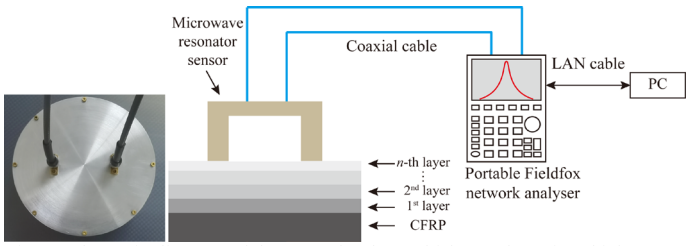

Fig. 4 Schematic diagram of the setup for the multi-layered coating thickness measurement with the open cavity resonator sensor.

The κ_1 values are close for both materials. Though the intercepts are not zero, they are much smaller than the dynamic range of the frequency shift. Thus, good agreement is shown between the theoretical analysis (i.e., (9)) and simulation.

The electric and magnetic field distributions in the coating at t=1 mm are shown in Fig. 7, where the patterns agree well with those of the TE_{011} mode. From the colorbar it is also indicated that little energy escapes from the cavity and the assumptions employed in the analytical modelling is verified. The effect of the sample size is also studied, and little change is seen in the resonance frequency when the sample size is larger than the diameter of the cavity aperture.

The cavity without the groove design is simulated. As shown in Fig. 8, more than one resonant peak exists and the response is asymmetrical. The distortion is caused by the significant interference of the degenerate mode, making it difficult to determine the resonance frequency shift. Therefore, the necessity of applying the grooves is well demonstrated.

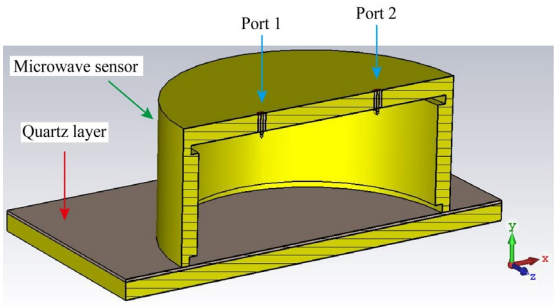

(a)

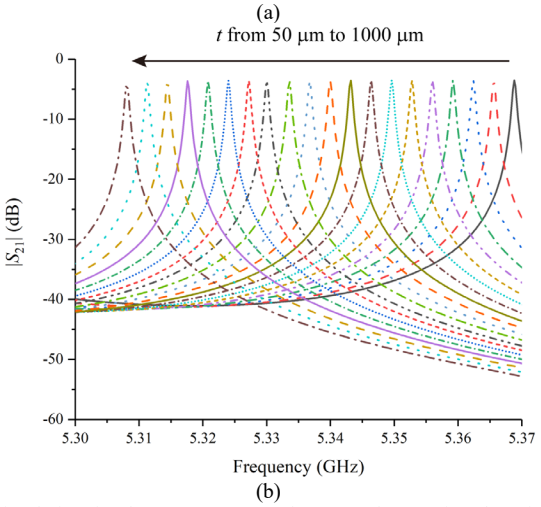

(b)

Fig. 5 Simulation for the measurement of a quartz layer using the microwave resonator sensor: (a) cross sectional view of the simulation model; (b) signal responses.

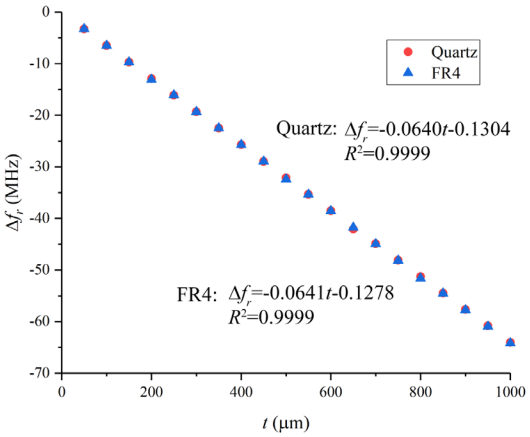

Fig. 6 Variation of the resonance frequency shift simulated at different layer thicknesses.

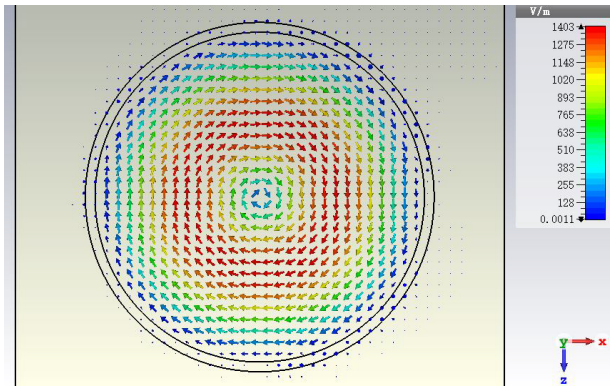

(a)

(b)

Fig. 7 Field distributions inside the 1 mm thick quartz layer: (a) electric field (relatively low field intensity out of the cavity); (b) magnetic field.

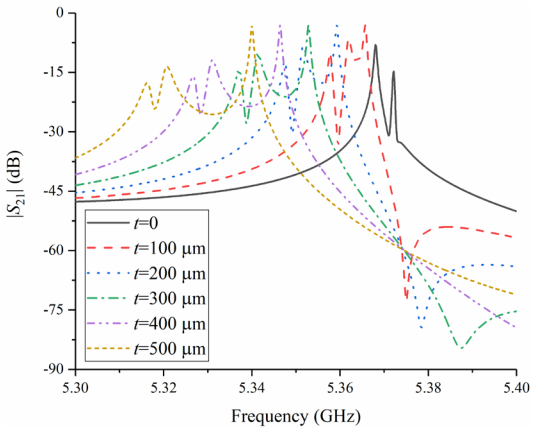

Fig. 8 Resonant responses simulated for the microwave sensor without grooves.

B. Experimental results

1) No-coating case

The sensor was directly placed on an aluminum plate and a plain woven composite plate. The frequency responses are given in Fig. 9. The resonance frequencies for the metal and woven composite are 0.1% and 0.2% lower than that of a closed cavity, respectively. It is indicated that an imperfect contact between the cavity wall and the sample produces a negligible effect. The reduced conductivity of the endplate lowers the resonance frequency value, which agrees with (4). However, the effect can be treated trivial. Therefore, similar to a metallic plate, a highly resonant system can still be formed with a low-conductivity composite, and the validity of using the perturbation theory for modelling is confirmed. The effect of the positioning on the composite plate is analyzed by rotating the composite over a range of 0º-90º with an interval of 15º. Given the small variation (± 5 MHz) of the resonance frequency, the composite is shown electrically isotropic.

2) One-layer coating case

Plain woven composite: Same as typical aircraft painting (0.05-0.5 mm) [22], here the total coating thickness was set low (less than 1.5 mm), i.e., up to 30 pieces for PE, 25 pieces for PET, four pieces for PVC and eight pieces for FR4. The resonance frequency changes with respect to the uncoated composite are presented in Fig. 10, where linear trends are observed. Three consecutive measurements were taken in each thickness case. Little variation was seen in the resonance frequency value due to the good repeatability of the sensor, so error bars are not provided in the figure. As listed in Table I, the differences between the κ_1 values by linear fitting are not appreciably large if the most significant digit is kept (i.e., -0.06). The finding is consistent with the theoretical modelling and simulation. It is also suggested that the presence of the small air gap between the sensor and coating in the tests does not have a significant effect, thereby enabling easy operation.

The performance of the TE_{012} mode is also evaluated using PET for comparison, as this higher mode can also be excited by the same coupling loop. The corresponding frequency shifts at different PET layer thicknesses are presented in Fig. 11. A linear relationship is seen, and this can be explained by the fact that the analytical model is not limited to a specific mode. It is noticed that the value of κ_1 is about twice that in the TE_{011} mode, due to the differences in the mode-dependent ξ. The normalized resonant responses in both modes are shown in Fig. 12. In the TE_{011} mode the shape of the curve does not significantly change with increasing thickness and the quality factors remain high (around 1850). However, in the TE_{012} mode the curve becomes flatter when the thickness increases, indicating a lower quality factor. For example, the quality factor decreases from 1070 for the PET-0 case to 364 for the PET-20 case. The effect of the higher mode is also reflected in the lower R^2 value. Hence, the TE_{011} mode better satisfies the small perturbation condition and better results can be provided.

UD composite: The UD composite has stronger conductivity anisotropy than the woven one. Hence, the variation of the resonance frequency shift is studied at different thicknesses and rotation angles. Taking PET as an example, as seen in Fig. 13, points for the seven rotation angles are closely spaced. For example, at t=840 μm, the difference between the largest and smallest frequency changes is within ±3%, demonstrating the insensitivity to the fiber directions. Linear fitting is also performed, and the average values of κ_1 and κ_0 are -0.0580 and 0.2008, respectively. The results are similar to those for the plain weave composite.

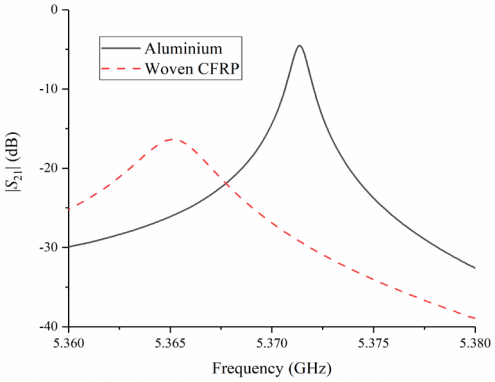

Fig. 9 Comparison of the signal responses for an aluminum plate and a woven composite substrate.

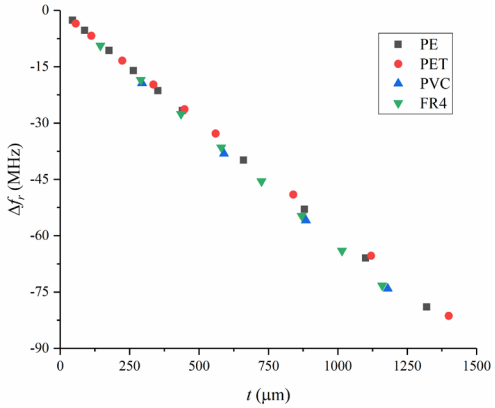

Fig. 10 Shift of the resonance frequency due to the increased thickness for one coating layer on a plain woven composite plate.

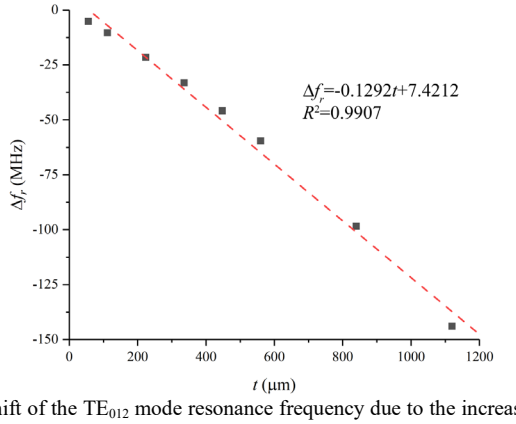

Fig. 11 Shift of the TE_{012} mode resonance frequency due to the increased PET layer thickness in the one-layer coating case.

TABLE I

REGRESSION CONSTANTS AND COEFFICIENTS OF DETERMINATION (R^2) FOR THE FITTING OF THE RESONANCE FREQUENCY SHIFT IN THE ONE-LAYER COATING CASE

	PE	PET	PVC	FR4
κ_1	-0.0598	-0.0580	-0.0617	-0.0628
κ_0	-0.1743	-0.3249	-1.3833	-0.1905
R^2	0.9999	0.9999	0.9999	0.9999

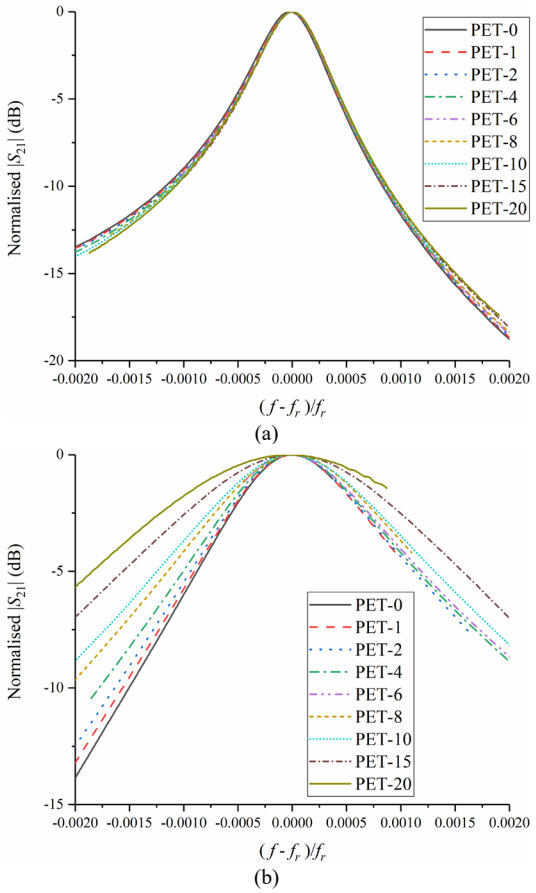

Fig. 12 Normalised S_{21} traces against changes in the fractional frequency at different PET layer thicknesses (PET-8 denotes eight PET pieces): (a)TE_{011} mode; (b)TE_{012} mode.

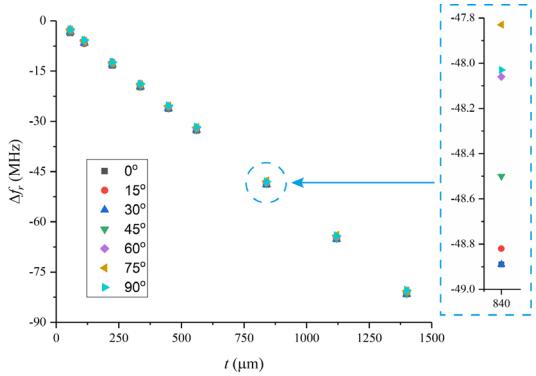

Fig. 13 Variation of the resonance frequency change for the unidirectional composite substrate at varied coating thicknesses and rotation angles in the one-layer coating case.

3) Two-layer coating case

For the two-layer case, PET and FR4 were used as primer and topcoat on the woven composite plate, respectively. The resonance frequencies for different thicknesses of PET and FR4 are listed in Table II. (10) is adopted here for the estimation of the total thickness, where case *a* corresponds to the composite only and case *b* corresponds to one PET layer on the composite (i.e., f_r=5.3619 GHz). Hence, the results of both cases are used as a form of calibration. As given in Table III, the errors of the thickness estimation are well within ±5%. For comparison, a simplified variant of (15) is adopted,

$$t = \Delta f_r / \kappa_1' \tag{16}$$

where κ_1'=-0.06 (average value of the κ_1 data in Table I) and the resonance frequency of the composite only case is used as the reference for the computation of Δf_r. This equation has the same form as (9). As presented in Table IV, the resultant prediction errors are within ±6%. Hence, it is suggested that the empirical κ_1' value can be used for rapid estimation as a first guess and reasonable results can be offered.

4) Multi-layered coating case

Same as the two-layer coating tests, here up to six layers of materials were measured on the woven composite plate. (10) is adopted for the thickness estimation, where case *a* corresponds to the composite only and case *b* corresponds to a two-layer case (i.e., PE\PET, where the material on the right of the backslash symbol is placed on top of that on the left). As listed in Table V, all the errors are well within ±2%, showing high accuracy. (16) also provides promising results with errors within ±3%.

C. Discussion

By substituting the field equations of the TE_{011} mode into (2) and (9b), the theoretical value of κ is calculated, i.e., κ= -0.0653. The computation process can be found in the appendix.

TABLE II

RESONANCE FREQUENCIES FOR VARIED COMBINATIONS OF PET (PRIMER) AND FR4 (TOPCOAT) PIECES ON THE WOVEN COMPOSITE PLATE (UNIT: GHz)

Number of PET pieces	Number of FR4 pieces: 1	2	3	4	5	6
1	5.3526	5.3435	5.3342	5.3250	5.3159	5.3067
2	5.3493	5.3399	5.3308	5.3218	5.3125	5.3032
5	5.3395	5.3304	5.3212	5.3121	5.3029	5.2936
10	5.3233	5.3141	5.3049	5.2958	5.2864	5.2768
15	5.3073	5.2980	5.2888	5.2793	5.2698	5.2600
20	5.2909	5.2814	5.2718	5.2623	5.2528	5.2425
25	5.2746	5.2650	5.2550	5.2449	5.2349	5.2249

TABLE III

PREDICTION ERRORS OF THE TOTAL THICKNESS FOR THE TWO-LAYER CASES USING (10) (UNIT: %)

Number of PET pieces	Number of FR4 pieces: 1	2	3	4	5	6
1	4.84	4.60	4.89	5.04	4.90	5.00
2	3.06	4.89	4.73	4.36	4.57	4.91
5	0.48	1.45	2.28	2.62	3.04	3.36
10	-1.09	-0.15	0.72	1.19	1.88	2.72
15	-2.26	-1.22	-0.41	0.52	1.28	2.15
20	-2.41	-1.27	-0.20	0.56	1.20	2.37
25	-2.65	-1.55	-0.29	0.90	1.82	2.63

Table IV

PREDICTION ERRORS OF THE TOTAL THICKNESS FOR THE TWO-LAYER CASES USING (16) (UNIT: %)

Number of PET pieces	Number of FR4 pieces: 1	2	3	4	5	6
1	5.31	5.07	5.35	5.51	5.37	5.47
2	3.52	5.36	5.20	4.83	5.04	5.38
5	0.93	1.90	2.74	3.08	3.50	3.82
10	-0.65	0.29	1.17	1.64	2.33	3.18
15	-1.82	-0.77	0.03	0.97	1.73	2.61
20	-1.98	-0.83	0.24	1.00	1.65	2.83
25	-2.21	-1.11	0.16	1.35	2.27	3.08

TABLE V

PREDICTION ERRORS FOR MULTI-LAYERED COATING CASES USING (10) AND (16)

Coating case (number of foil pieces in the square brackets)	Actual thickness (μm)	f_r (GHz)	(10)		(16)	
			Estimated thickness (μm)	Error (%)	Estimated thickness (μm)	Error (%)
Composite only	0	5.3653	-	-	-	-
PE\PET [2\2]	200	5.3531	-	-	-	-
PE\PET\PVC [2\2\1]	495	5.3349	499.76	0.96	506.53	2.33
PE\PET\PVC\FR4 [2\2\1\1]	640	5.3257	650.84	1.69	659.65	3.07
PE\PET\PVC\FR4\PET [2\2\1\1\2]	752	5.3193	756.01	0.53	766.25	1.89
PE\PET\PVC\FR4\PET\PE [2\2\1\1\2\2]	840	5.3144	836.59	-0.41	847.92	0.94

The value of κ is close to that given by the simulation with an aluminum plate (Fig. 6), i.e., errors of -1.99% and -1.84% for quartz and FR4, respectively. In addition, compared with the experimental results of the one-coating case (Table I), the differences for FR4, PVC, PE and PET are -3.83%, -5.51%, -8.42% and -11.18%, respectively. The slightly higher discrepancy is caused by the simplification adopted in the modelling, where the power loss in the substrate is not considered. Thus, it is verified that for a low-conductivity substrate the use of an empirical κ value instead of a theoretical value is more appropriate for coating thickness estimation.

Similarly, for the TE_{012} mode, the theoretical value of κ=-0.1667 is obtained, and a larger difference of around -22.50% with the experiment is observed, indicating even greater energy dissipation. Therefore, it is suggested that the analytical model proposed becomes not accurate enough for this mode. This is another reason that the TE_{011} mode is more desired.

VI. Concluding Remarks

A novel methodology has been presented for accurate coating thickness measurement on carbon fiber composite plates using an open microwave cavity resonator sensor. Incorporating the cavity perturbation technique, the analytical model proposed can be applied to multi-layered coating cases. It has been found that the resonance frequency shift is proportional to the coating thickness. The measurement is insensitive to the coating and substrate types, facilitating convenient use in the field. The findings agree well with the electromagnetic simulation and experimental results. For the thickness estimation, the resonance frequencies in two reference cases can be used, and estimation errors within ±5% have been provided. Alternatively, an empirical κ value (i.e., -0.06) can be adopted for the prediction as a first guess. For near future work, a wider range of coating thicknesses and materials will be thoroughly examined to suit applications in other fields, and a low-cost microwave circuit with a short frequency bandwidth will be designed. The efficacy for real coated aircraft composite structures will be examined.

APPENDIX

For a cylindrical cavity shown in Fig. A1, the fields of the $TE_{01\ell}$ mode in a cylindrical cavity resonator can be written as

$$H_z = H_0 J_0\left(\frac{p'_{01}\rho}{a}\right)\sin\frac{\ell\pi z}{h} \tag{A1a}$$

$$H_\rho = \frac{\beta a H_0}{p'_{01}} J'_0\left(\frac{p'_{01}\rho}{a}\right)\cos\frac{\ell\pi z}{h} \tag{A1b}$$

$$H_\varphi = 0 \tag{A1c}$$

$$E_\rho = 0 \tag{A1d}$$

$$E_\varphi = \frac{jk\eta a H_0}{p'_{01}} J'_0\left(\frac{p'_{01}\rho}{a}\right)\sin\frac{\ell\pi z}{h} \tag{A1e}$$

$$E_z = 0 \tag{A1f}$$

where H_0 is a constant. $\eta=\sqrt{\mu/\varepsilon}$ is the intrinsic impedance of the material (with the electric permittivity ε and magnetic permeability μ) filling the cavity. For the air-filled cavity developed here, ε and μ are close to the permittivity and permeability of free space. Thus, η is equal to the impedance of free space, i.e., 376.7 Ω). a and h are the radius and height of the cavity, respectively. k and β are the wave number and propagation constant of the standing waves, respectively, and they are defined as

$$k = \frac{\omega}{c} \tag{A2a}$$

$$\beta = \sqrt{k^2 - \left(\frac{p'_{01}}{a}\right)^2} \tag{A2b}$$

where $\omega=2\pi f$ is the angular frequency and f is the frequency in Hz. c is the speed of light in free space.

Using (A1a-1f), the numerator and denominator of (2) can be calculated by

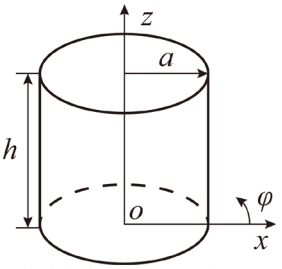

Fig. A1 Geometry of a cylindrical resonant cavity.

$$\int_s \left|\bar{H}\right|^2 ds = \int_{\phi=0}^{2\pi}\int_{\rho=0}^{a}\left|H_\rho\left(z=0\right)\right|^2 \rho d\rho d\phi$$
$$= \frac{\beta^2 a^2 H_0^2}{\left(p'_{01}\right)^2}\cdot\int_{\phi=0}^{2\pi} d\phi\cdot\int_{\rho=0}^{a} J_0'^2\left(\frac{p'_{01}\rho}{a}\right)\rho d\rho \qquad \text{(A3a)}$$
$$= \frac{\pi\beta^2 a^4 H_0^2}{\left(p'_{01}\right)^2} J_0^2\left(p'_{01}\right)$$

$$\int_V \left(\varepsilon\left|\bar{E}\right|^2 + \mu\left|\bar{H}\right|^2\right) dv = 2\int_V \varepsilon\left|\bar{E}\right|^2 dv$$
$$= 2\int_{z=0}^{h}\int_{\phi=0}^{2\pi}\int_{\rho=0}^{a}\left|E_\phi\right|^2 \rho d\rho d\phi dz$$
$$= \frac{k^2\eta^2 a^2 H_0^2}{\left(p'_{01}\right)^2}\cdot\int_{\phi=0}^{2\pi} d\phi\cdot\int_{z=0}^{h}\left(\sin\frac{\ell\pi z}{h}\right)^2 dz \qquad \text{(A3b)}$$
$$\cdot\int_{\rho=0}^{a} J_0'^2\left(\frac{p'_{01}\rho}{a}\right)\rho d\rho$$
$$= \frac{\pi k^2\eta^2 a^4 H_0^2 h}{\left(p'_{01}\right)^2} J_0^2\left(p'_{01}\right)$$

The characteristic that the time-average stored electric and magnetic energies are equal at resonance is used in the deduction. Therefore, ξ can be expressed as

$$\xi = \frac{1}{\mu_0 h}\left[1-\left(\frac{cp'_{01}}{2\pi fa}\right)^2\right] \qquad \text{(A4)}$$

Further, κ can be given by

$$\kappa = -\frac{\xi Z_0 f}{c} = -\frac{Z_0 f}{\mu_0 hc}\left[1-\left(\frac{cp'_{01}}{2\pi fa}\right)^2\right] \qquad \text{(A5)}$$

The parameter ℓ is not shown in the expression, while it is reflected in the resonance frequency f (see (14)). By substituting the cavity dimensions and ℓ, the theoretical values of κ for the TE_{011} and TE_{012} modes are -0.0653 MHz/μm and -0.1667 MHz/μm, respectively.

ACKNOWLEDGMENT

The first author gratefully acknowledges Prof. Yang Ju (Nagoya University, Japan) for many useful discussions. Special thanks to Dr.Fei Fei for assistance in the experiments.

REFERENCES

[1] C. Soutis, “Fibre reinforced composites in aircraft construction,” *Prog. Aerosp. Sci.*, vol. 41, no. 2, pp. 143–151, 2005.

[2] J. C. Brasunas, G. M. Cushman, and B. Lakew, “Thickness Measurement,” in *Measurement,Instrumentation, and Sensors Handbook*, 2nd ed., J. G. Webster and H. Eren, Eds. Boca Raton: CRC Press, 1999, p. 3559.

[3] B. Cao, M. Wang, X. Li, M. Fan, and G. Tian, “Noncontact Thickness Measurement of Multilayer Coatings on Metallic Substrate Using Pulsed Terahertz Technology,” *IEEE Sens. J.*, vol. 20, no. 6, pp. 3162–3171, 2020.

[4] S. K. Jain, P. P. Gupta, and A. C. Eapen, “An X-ray fluorescence method for coating thickness measurement,” *X-Ray Spectrom.*, vol. 8, no. 1, pp. 11–13, Jan. 1979.

[5] Z. Li, P. Wang, A. Haigh, C. Soutis, and A. Gibson, “Review of microwave techniques used in the manufacture and fault detection of aircraft composites,” *Aeronaut. J.*, vol. 125, no. 1283, pp. 151–179, Jan. 2021.

[6] K. Brinker, M. Dvorsky, M. T. Al Qaseer, and R. Zoughi, “Review of advances in microwave and millimetre-wave NDT&E: principles and applications,” *Philos. Trans. R. Soc. A Math. Phys. Eng. Sci.*, vol. 378, no. 2182, p. 20190585, Oct. 2020.

[7] Z. Li, A. Haigh, C. Soutis, and A. Gibson, “Principles and Applications of Microwave Testing for Woven and Non-Woven Carbon Fibre-Reinforced Polymer Composites: a Topical Review,” *Appl. Compos. Mater.*, vol. 25, no. 4, pp. 965–982, Aug. 2018.

[8] R. Zoughi, J. R. Gallion, and M. T. Ghasr, “Accurate Microwave Measurement of Coating Thickness on Carbon Composite Substrates,” *IEEE Trans. Instrum. Meas.*, vol. 65, no. 4, pp. 951–953, 2016.

[9] J. S. Takeuchi, M. Perque, P. Anderson, and E. G. Sergoyan, “Microwave paint thickness sensor,” US 7898265, 2011.

[10] J. Hinken, “Device for measuring coating thickness,” US 9395172, 2016.

[11] Z. Li, Z. Meng, C. Soutis, A. Haigh, P. Wang, and A. Gibson, “Bimodal Microwave Method for Thickness Estimation of Surface Coatings on Polymer Composites,” *Adv. Eng. Mater.*, p. 2100494, Aug. 2021.

[12] C. Brandt, W. Bisle, J. Dannemann, J. Hinken, and T. Beller, “Device for the measurement of coating thickness by means of microwaves,” US 8866496 B2, 2014.

[13] S. Donovan, O. Klein, M. Dressel, K. Holczer, and G. Grüner, “Microwave cavity perturbation technique: Part II: Experimental scheme,” *Int. J. Infrared Millimeter Waves*, vol. 14, no. 12, pp. 2459–2487, Dec. 1993.

[14] O. Klein, S. Donovan, M. Dressel, and G. Grüner, “Microwave cavity perturbation technique: Part I: Principles,” *Int. J. Infrared Millimeter Waves*, vol. 14, no. 12, pp. 2423–2457, Dec. 1993.

[15] L. F. Chen, C. K. Ong, C. P. Neo, V. V. Varadan, and V. K. Varadan, *Microwave Electronics: Measurement and Materials Characterization*. Chichester, UK: John Wiley & Sons, Ltd, 2004.

[16] R. E. Collin, *Foundations for Microwave Engineering*, 2nd ed. Wiley-IEEE Press, 2000.

[17] T. Y. Otoshi, R. Cirillo, and J. Sosnowski, “Measurements of Complex Dielectric Constants of Paints and Primers for DSN Antennas: Part I,” California, 1999.

[18] E. P. Emilsson, “Radar Transparency and Paint Compatibility,” Chalmers University of Technology, 2017.

[19] Z. Li, A. Haigh, C. Soutis, and A. Gibson, “X-band microwave characterisation and analysis of carbon fibre-reinforced polymer composites,” *Compos. Struct.*, vol. 208, pp. 224–232, Jan. 2019.

[20] S. Horn, “Parylene Dielectric Properties,” 2015.

[Online].Available:https://blog.paryleneconformalcoating.com/parylene-dieletric-properties/.[Accessed:02-Sep-2021].

[21] D. M. Pozar, *Microwave Engineering*, Fourth edi. New York: John Wiley & Sons, 2012.

[22] F. Moupfouma, "Aircraft Structure Paint Thickness and Lightning Swept Stroke Damages," *SAE Int. J. Aerosp.*, vol. 6, no. 2, pp. 2013-01–2135, Sep. 2013.

Zhen Li received his B.S. and M.S. degrees in aerospace engineering from Nanjing University of Aeronautics and Astronautics, Nanjing, China in 2010, and Shanghai Jiao Tong University, Shanghai, China in 2013, respectively, and the Ph.D. degree in materials from The University of Manchester, UK, in 2017. He is currently an Associate Professor with College of Automation Engineering, Nanjing University of Aeronautics and Astronautics, Nanjing, China. His research interests include advanced sensors and instrumentation, microwave nondestructive testing and electromagnetics.

Changcheng Wu received his B.S. and Ph.D. degree in Instrument science and technology from Jilin University, Jilin, China in 2010, and Southeast University, Nanjing, China in 2016, respectively. He is currently an associate professor with Nanjing University of Aeronautics and Astronautics, Nanjing, China. His research interests include advanced sensor techniques and wearable devices.

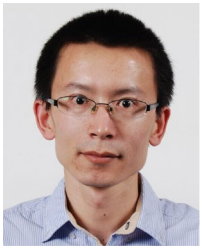

Zhaozong Meng received his B.S. and M.S. degrees in measurement and control technology and instrument from Sichuan University, Chengdu, China in 2006, and Beihang Univerisity, Beijing, China in 2009, respectively, and his Ph.D. degree in computer science from University of Huddersfield, West Yorkshire, UK, in 2014. He is currently an associate professor with School of Mechanical Engineering, Hebei University of Technology, Tianjin, China. His research interests include advanced sensor techniques, wearable devices, industrial IoT and cyber-physical systems.

Constantinos Soutis received his B.S. and and M.S. degrees in Aeronautics from the University of London Queen Mary College and Imperial College London, respectively, and Ph.D. degree from Cambridge University. He is currently working at the University of Manchester as Chair of Aerospace Engineering and Director of the Aerospace Research Institute. Professor Soutis is a Fellow of the Royal Academy of Engineering. His research interests include the science and technology of the mechanics and mechanisms of failure of fiber-composite materials.

Zhijun Chen received his B.S. degree in instrumentation engineering from Hubei University of Technology, Wuhan, China in 1997, M.S. degree in solid mechanics from Zhejiang University of Technology, Hangzhou, China in 2003, and the Ph.D. degree in instrument science and technology from Shanghai Jiao Tong University, Shanghai, China in 2008. He is currently an Associate Professor with College of Automation Engineering, Nanjing University of Aeronautics and Astronautics, Nanjing, China. His research interests include acoustic wave sensors and ultrasonic nondestructive testing.

Ping Wang received his B.S. and Ph.D. degree in Instrument science and technology from Southeast University, Nanjing, China, in 1999 and 2004, respectively. He is currently a full professor with Nanjing University of Aeronautics and Astronautics, Nanjing, China. His research interests include advanced sensor techniques and nondestructive testing.

Andrew Gibson (M'03–SM'06) received his M.Eng. and Ph.D. degrees in electrical and electronic engineering from Heriot-Watt University, Edinburgh, U.K., in 1985 and 1988, respectively, and the D.Sc. degree from the University of Manchester Institute of Science and Technology (UMIST), Manchester, U.K., in 2003. He was General Chairman of European Microwave Week 2016. He is currently the Pro-Vice-Chancellor of Manchester Metropolitan University, U.K. He specializes in the application of microwave sensors to food characterizations and microwave materials measurements. He is a Fellow of the Institute of Engineering and Technology.